ORIGINAL ARTICLE

The creation of a neural network based capability profile to enable generative design and the manufacture of functional FDM parts

Mark Goudswaard[1] · Ben Hicks[1] · Aydin Nassehi[1]

Abstract
In order to manufacture functional parts using filament deposition modelling (FDM), an understanding of the machine's capabilities is necessary. Eliciting this understanding poses a significant challenge due to a lack of knowledge relating manufacturing process parameters to mechanical properties of the manufactured part. Prior work has proposed that this could be overcome through the creation of capability profiles for FDM machines. However, such an approach has yet to be implemented and incorporated into the overall design process. Correspondingly, the aim of this paper is two-fold and includes the creation of a comprehensive capability profile for FDM and the implementation of the profile and evaluation of its utility within a generative design methodology. To provide the foundations for the capability profile, this paper first reports an experimental testing programme to characterise the influence of five manufacturing parameters on a part's ultimate tensile strength (UTS) and tensile modulus (E). This characterisation is used to train an artificial neural network (ANN). This ANN forms the basis of a capability profile that is shown to be able to represent the mechanical properties with RMSEP of 1.95 MPa for UTS and 0.82 GPa for E. To validate the capability profile, it is incorporated into a generative design methodology enabling its application to the design and manufacture of functional parts. The resulting methodology is used to create two load bearing components where it is shown to be able to generate parts with satisfactory performance in only a couple of iterations. The novelty of the reported work lies in demonstrating the practical application of capability profiles in the FDM design process and how, when combined with generative approaches, they can make effective design decisions in place of the user.

Keywords Additive manufacture · Design for additive manufacture · Generative design · Capability profiles · Mechanical testing · Neural networks

1 Introduction

Additive manufacturing (AM) technologies afford a wide range of benefits over traditional manufacturing techniques. These include facilitating increased design freedoms [1], reducing manufacturing costs [2, 3] and minimising both part weight and waste during production [4]. These benefits are enabled in part by the large range of manufacturing parameters that can be individually controlled when generating manufacturing tool paths. A number of these parameters are shown in Fig. 1.

Of the technologies available, the most widely used in the consumer market is filament deposition modelling (FDM), accounting for 69% of 3D printing technologies [6]. In addition to the general benefits afforded by AM, FDM can also enable the affordable manufacture of parts in homes and communities, and in doing so can eliminate the need for supply chains [7].

These design freedoms, however, are not without their pitfalls. A key issue associated with them is a product of the FDM design space being very large and, at present, insufficiently understood [8]. As a result, the manufacture of parts with predictable mechanical properties is at best very difficult
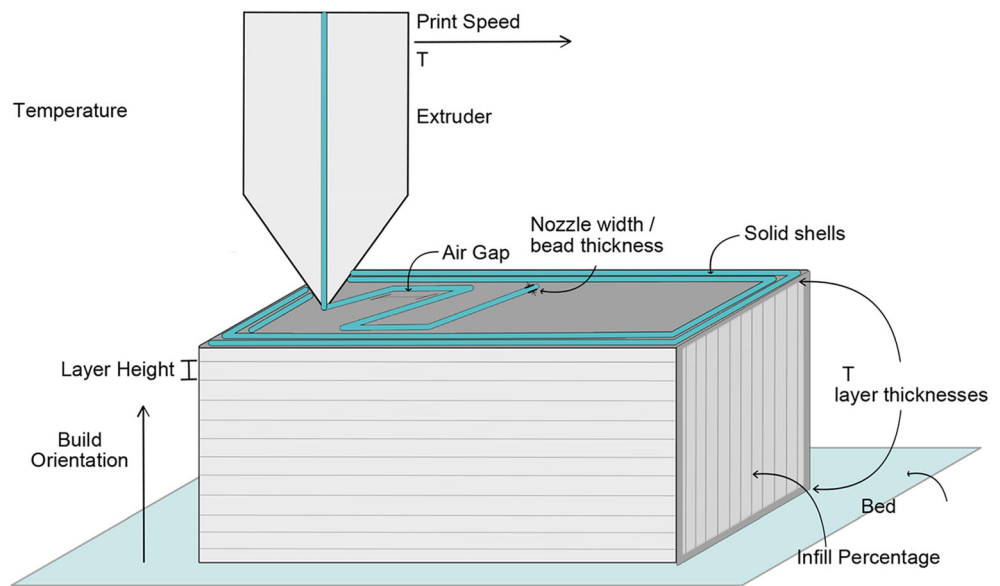
✉ Mark Goudswaard
  Mark.goudswaard@bristol.ac.uk

  Ben Hicks
  Ben.hicks@bristol.ac.uk

  Aydin Nassehi
  Aydin.nassehi@bristol.ac.uk

1 Department of Mechanical Engineering, University of Bristol, Queen's Building, University Walk, Bristol BS8 1TR, UK

Fig. 1 Manufacturing parameters that can be varied with the FDM process (adapted from [5])

(for someone familiar with FDM and a specific printer) and at worst impossible for someone without this knowledge of FDM and its particularities.

It was previously proposed that this could be addressed through the generation and implementation of capability profiles for FDM [9]. Through their use, the manufacture of parts with reliable properties could be enabled.

Correspondingly, the aims of this paper are to create a comprehensive capability profile for FDM and apply it within a generative design methodology to validate its utility and to deduce whether it can enable the creation of functional components. In meeting this aim, it provides three key contributions. First, it presents mechanical testing of 3D-printed specimens and identifies trends between manufacturing parameters and mechanical properties (contribution 1). Second, it uses this empirical data to train an artificial neural network which is subsequently used as a capability profile (contribution 2). Third, to demonstrate the utility of the capability profile, it is implemented within a generative design methodology which is used in the design and manufacture of two load bearing components (contribution 3).

The remainder of this paper is structured as follows. First, an overview of FDM manufacturing parameters is given and the impact they have on the mechanical properties of printed parts is outlined. Second, how capability profiles could be used to address this is presented and, based upon this, key manufacturing parameters are identified for inclusion within the capability profile. Third, a mechanical testing program is undertaken to provide empirical data to train a neural network and subsequently underpin the capability profile. Fourth, the creation of the capability profile is presented. The capability profile's use within a generative design methodology is then demonstrated. Finally, the practical use of both the methodology and the incorporated capability profile is shown. The

discussion section considers the learnings and limitations of the overall approach and the results and processes employed at each stage.

2 Background

To contextualise the work carried in this paper, this section will consider three areas: material testing for FDM, capability profiling and generative design in the context of additive manufacturing. In doing this, it will clarify the four research gaps that the paper will address.

2.1 Material testing for FDM

A number of extant studies in literature have sought to elucidate the impacts that different manufacturing parameters have upon the mechanical properties of 3D-printed parts. The directives for a number of relationships have been elicited and can be summarised as follows:

1. It has generally been shown that smaller layer heights increase part strength [10–15] but some studies demonstrate the contrary with positive correlations [16]. Chacón et al. found both negative and positive correlations dependent upon build orientation [17].
2. Studies of part build orientation have revealed that parts are anisotropic and are found to be weakest in the direction of build (Z-direction) [10, 11, 13, 16–19].
3. Parts are shown to be strongest when the raster angle is in the direction of the applied load and increased raster width increases part strength [11, 13, 18–20] and a negative air gap between rasters is found to increase part strength [11, 18, 19].

4. An increased infill percentage is found to increase part strength [16] as is also observed when increasing the number of solid shells [13, 18].
5. Extrusion temperature is shown to significantly impact the mechanical properties of the printed parts with distinct optimum extrusion temperature ranges existing for different materials [16, 21, 22].
6. When the same printer and manufacturing parameters are used, mechanical properties of parts are found to vary significantly with material type [10, 11] and colour [21]. Identical parts manufactured with the same manufacturing parameters, same material and on the same material are shown to have variability in UTS of up to 26% [23].

Whilst the directives for a number of relationships have been deduced in existing literature, these take place with a wide variety of printers, polymers, slicing software and process parameters. As a result, generalising trends from these results is very difficult [8] and, consequentially, these existing test results cannot be used as a basis for a capability profile. This forms the basis of the first research gap that this paper seeks to address by undertaking comprehensive testing on a single printer with a consistent material to permit the generation a usable capability profile.

2.2 Capability profiling

Capability profiles relate the impact that machining or manufacturing parameters have on part properties by accounting for changes to a manufacturing resource over time. They can be considered to be time-sensitive images of a manufacturing resource, representing the capabilities that a specific machine tool will be able to provide at a specific time on a specific product [24]. By combining this with information about a part's geometry and stock material, a part's characteristics can be described. This can take place at levels ranging from the geometry of an element to the chemical integration at the atomic scale [25].

In traditional manufacturing processes, capability profiles have been used to provide tool health data models [26], optimise the generation of process plans [24] and to predict performance of cutting, grinding and turning [25, 27].

With respect to the use of capability profiles for FDM, a framework for their incorporation in the design for additive manufacture process is presented in existing literature by the authors [9]. Within this, the parameters that would need to be included within a capability profile are extrusion temperature, material type, variability, raster angle, infill pattern, raster width, infill percentage, top/bottom layers, solid shells, layer height and build orientation.

A number of existing studies have sought to create predictive models for FDM printing based upon empirical data. Group method of data handling was used by Onwubolu

et al. to generate a model using layer thickness, part orientation, raster width and air gap [11]. This, however, used only two levels for each parameter meaning only linear relationships could be deduced. An analytical model was used by Croccolo et al. to predict tensile strength based upon build orientation and number of solid shells [18]. A wide range of machine learning techniques have been used in AM [28]. Artificial neural networks (ANNs) were used by Sood et al. [12] to predict compressive strength based upon layer thickness, build orientation, raster angle, raster width and air gap. ANNs were also used by Garzon-Hernandes et al. who present a two-stage thermal sintering method for predicting the mechanical performance of ABS samples [15]. Zhang et al. applied ANNs to predict mechanical properties based upon three process parameters with additional thermal data from the printing process [29].

These existing studies have been validated via their ability to predict the values of the data used to train them, and whilst they have shown good correlation, they have not been used to generate actual parts. They also omit a number of parameters that are considered to be necessary in a capability profile for FDM. As such, to build on previous related work, this addresses two further research gaps—to incorporate parameters not included in the capability profiles presented in previous work and to validate the performance of the generated capability profile in the creation of a functional component.

2.3 Generative design in the context of additive manufacturing

Generative design is a subset of assisted creation which refers to a wide range of tools that exist to assist humans in creative tasks [30] and can enable people to be 'more creative more of the time' [31].

Generative design itself is about designing not only the object but a process to generate objects [32]. A number of commercial design packages providing generative design capability exist, including the generative design environment within Autodesk's Fusion 360 [33]. An alternative is Paramate–a generative/parametric design service [34] that parameterises design processes for products that can be instantiated to individual requirements.

In the context of additive manufacturing, generative approaches are able to leverage the individually controllable manufacturing parameters to create parts with bespoke properties. Extant AM-specific generative approaches include methods for topological optimisation [35], part design based upon required motion profiles [36], optimising manufacturing parameters for balance [37] or moment of inertia [38]. None, however, have sought to enable the generation of dimensions and manufacturing parameters of load-bearing components for specific functional requirements. Correspondingly, the final research gap that this paper seeks to address is to

implement the capability profile in a generative design approach that can create parts to withstand specific loads.
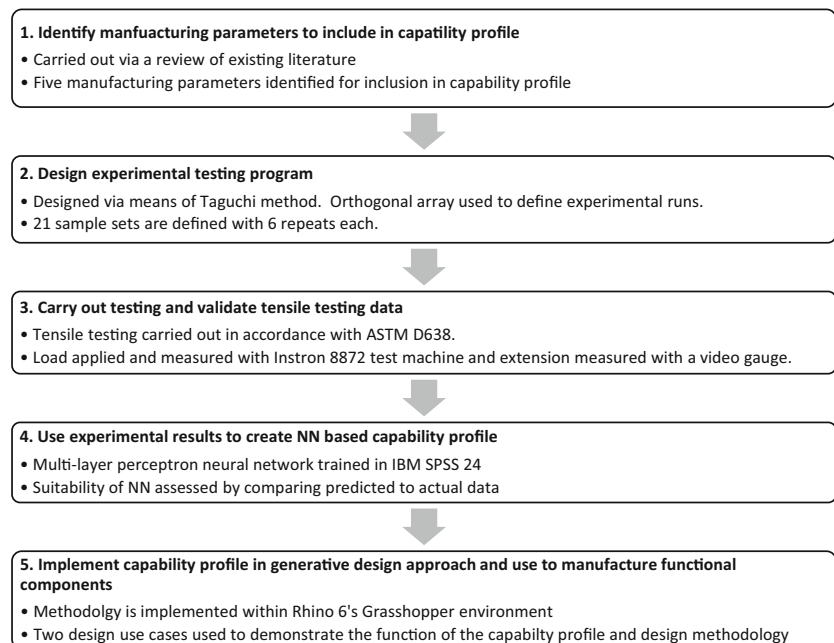
2.4 Summary

The reviewed literature has highlighted research gaps shaping the need to (i) conduct comprehensive testing on a single printer, (ii) incorporate parameters previously omitted from extant capability profiles for FDM, (iii) validate the behaviour of a capability profile by applying it in the creation of functional components and (iv) implement the capability profile within a generative design approach. These gaps shape the aim of the paper: to create a comprehensive capability profile for FDM and apply it within a generative design methodology to validate its utility and to deduce whether it can enable the creation of functional components.

3 Research methodology

As stated in Section 1, the aim of this paper is to research, create and implement a capability profile for FDM. An overview of the research methodology developed to achieve this is depicted in Fig. 2 and summarised in the following paragraphs.

First, based upon the results in literature, it is necessary to identify the parameters that will be included in the capability profile. The selection of parameters is based upon those found to significantly impact a part's mechanical performance (as per Section 2.1) and generally need to be manually selected by a user when creating manufacturing tool paths.

Having selected the parameters to include, a Taguchi design of experiments approach is used to determine parameter levels and define the 21 sets of parameter combinations to be tested.

Tensile testing is then carried out on the selected sample sets in accordance with ASTM standard D638. Testing is carried out on 120 specimens using an Instron 8872 and video gauge measuring equipment. The validity of the data is confirmed by ascertaining whether trends in the experimental data are congruent with those from literature.

The generated experimental data is then used to train a multi-layer perceptron neural network in IBM SPSS 24. Verification of the suitability of this as a capability profile is carried out by comparing predicted to actual loads for the data generated in the experimental testing.

This capability profile is then implemented within a generative design methodology and implemented in Rhino 6's Grasshopper environment. This permits the performance and functionality of the capability profile to be validated through the design of two functional components and in doing so it permits validation of the method employed to generate it.

The paper will reflect on all elements of the paper including the experimental method followed, the suitability of neural networks and the utility of capability profiles in design support tools.

4 Experimental testing

This section outlines the experimental testing procedure and results. As shown in Section 2.1, a range of manufacturing

Fig. 2 Methodology followed in paper

1. Identify manfuacturing parameters to include in capatility profile
- Carried out via a review of existing literature
- Five manufacturing parameters identified for inclusion in capability profile

2. Design experimental testing program
- Designed via means of Taguchi method. Orthogonal array used to define experimental runs.
- 21 sample sets are defined with 6 repeats each.

3. Carry out testing and validate tensile testing data
- Tensile testing carried out in accordance with ASTM D638.
- Load applied and measured with Instron 8872 test machine and extension measured with a video gauge.

4. Use experimental results to create NN based capability profile
- Multi-layer perceptron neural network trained in IBM SPSS 24
- Suitability of NN assessed by comparing predicted to actual data

5. Implement capability profile in generative design approach and use to manufacture functional components
- Methodolgy is implemented within Rhino 6's Grasshopper environment
- Two design use cases used to demonstrate the function of the capabilty profile and design methodology

parameters directly impact mechanical performance of FDM parts. Experimental characterisation of these in existing literature has taken place with a wide range of printers, materials and settings. This therefore presents a research gap which can be addressed by undertaking comprehensive testing for a wide range of parameters on a single printer with consistent material. The testing results also permit the formation of a capability profile for FDM.

4.1 Design of experiment

The parameters selected and the reasoning (according to reviewed literature in Section 2.1) for their inclusion within the capability profile are

- Layer height—as the impact of this parameter on mechanical properties was inconclusive.
- Build orientation—because of the demonstrated part anisotropy.
- Infill percentage—shown to significantly impact mechanical properties.
- Top/bottom layers—as it enables custom distribution of material through a part to achieve bespoke properties.
- Solid shells—same reasoning as for top/bottom layers.

In addition to these reasons, the chosen parameters frequently need to be selected by the user when generating tool paths.

All parameters were tested at three levels to permit elucidation of any non-linear relationships. The selected levels are shown in Table 1. These levels were chosen in such a way as to account for interdependencies between the parameters. For example, layer height must be a factor of all increments of top/bottom layer thickness.

In addition to those shown in Table 1, additional print parameters were kept consistent with those in Ultimaker Cura's 'normal' print profile. These consisted of a nozzle width of 0.4 mm, a grid infill pattern, general print speed of 60 mm/s, reduced print speed of 30 mm/s for walls, travel speed of 120 mm/s, build plate temperature of 60 °C and extruder temperature of 200 °C.

The Taguchi method permits robust and repeatable exploration of a solution space without needing to undertake a full-factorial experimental regime [39]. Because of this, it was used to define the parameter combinations used in experimental testing. A Taguchi orthogonal array for five variables at three levels is used to define the experimental runs to be undertaken [40]. This is shown in Table 2. The selected Taguchi array defines experimental runs 1–18. It was initially thought that these would be used as training data, with three further runs (19–21) included to be used for validation. However, as neural networks were used later for generating the capability profile all of the experimental data was pooled together and training, test and holdout data were selected when creating the neural network.

The necessary number of repeat tests for each parameter set is five as defined by the ASTM test standard [41]. Samples were manufactured in batches of six to allow for a single sample to be disregarded in the case of manufacturing defects or testing errors.

4.2 Tensile test method

The experimental test set-up consisted of a tensile test machine, video gauge and test lamp for illuminating the test specimen. These are all shown in Fig. 3.

The tensile tests were carried out on a 25 kN Instron 8872 test machine in accordance with ASTM D638 [41]. Testing was carried out across multiple days over the course of approximately a week. Depending on the test days, the machines were fitted with either 5 kN or 10 kN load cells. All tests were carried out with break loads within the recommended ranges for the load cells. Specimens were extended at a rate of 1 mm/min until failure. Instron's Wave Matrix software was used to execute the testing and export values of applied load.

Extension was measured using an iMetrum video gauge and software. This was used to track the distance between a set of points at either end of the reduced section of the test specimen. The tracking points are shown in Fig. 4 for a specimen mid-test. The iMetrum software receives the load output from the Instron machine in real time and combines them with measured extension to provide load, extension values from the tests. These values were analysed in Excel and MATLAB. Test videos were also exported. Two stills from these are shown in Fig. 4 demonstrating a test specimen pre- (Fig. 4a) and post-test (Fig. 4b), respectively.

The test specimen used is adapted from the ASTM standard specimen types. This was necessary to accommodate the defined values of the independent variables and to be of large enough size such that enough increments of solid shells and top/bottom layers (as shown in Table 1) whilst also being short enough to permit it to be printed reliably in the upright Z orientation. Accordingly, specimen thickness was increased from 3.2 to 4 mm, width increased from 6 to 8 mm and specimen overall reduced from 183 to 140 mm. The specimen's major dimensions are shown in Fig. 5.

Table 1 Manufacturing parameters and levels

Parameter	Level 1	Level 2	Level 3
Layer height (mm)	0.1	0.2	0.3
Build orientation	X	Y	Z
Infill percentage (%)	20	60	100
Top/bottom layers (mm)	0.6	1.2	1.8
Solid shells (mm)	0.4	1.2	2

Table 2 Taguchi orthogonal array demonstrating parameter combinations for experimental testing. Levels correspond to those defined in Table 1

| Sample | Levels | | | | |
	Layer height	Infill percentage	Top/bottom layers	Solid shells	Build orientation
1	1	1	1	1	1
2	1	2	2	2	2
3	1	3	3	3	3
4	2	1	1	2	2
5	2	2	2	3	3
6	2	3	3	1	1
7	3	1	2	1	3
8	3	2	3	2	1
9	3	3	1	3	2
10	1	1	3	3	2
11	1	2	1	1	3
12	1	3	2	2	1
13	2	1	2	3	1
14	2	2	3	1	2
15	2	3	1	2	3
16	3	1	3	2	3
17	3	2	1	3	1
18	3	3	2	1	2
19	2	2	2	2	2
20	1	1	2	3	1
21	3	3	2	1	3

5 Results

Results of the tests are shown in Table 3. These show the measured parameters of cross-sectional area, break load and extension in mm.

Three calculated parameters are also shown. UTS is calculated as the max load divided by the cross-sectional area. Strain at UTS is calculated as extension divided by gauge length expressed as a percentage.

Tensile modulus (E) was determined from the slope of the linear portion of the stress-strain curve.

Figure 6a and b show the stress-strain graphs for parameter sets 1 and 14, respectively. They demonstrate the typical curves obtained and also the consistency of results.

5.1 Identification of trends

From the experimental testing results, trends could be elucidated with respect to the impact each parameter had on the UTS and tensile modulus, respectively. These were deduced by calculating the normalised effect of each variable in accordance with the Taguchi method [39]. In accordance with the Taguchi method, the trends are represented as vectors between data points.

Fig. 3 Experimental set-up for tensile testing

Fig. 4 Stills from video gauge footage—**a** points used for extension tracking, **b** specimen post-test demonstrating failure in reduced section

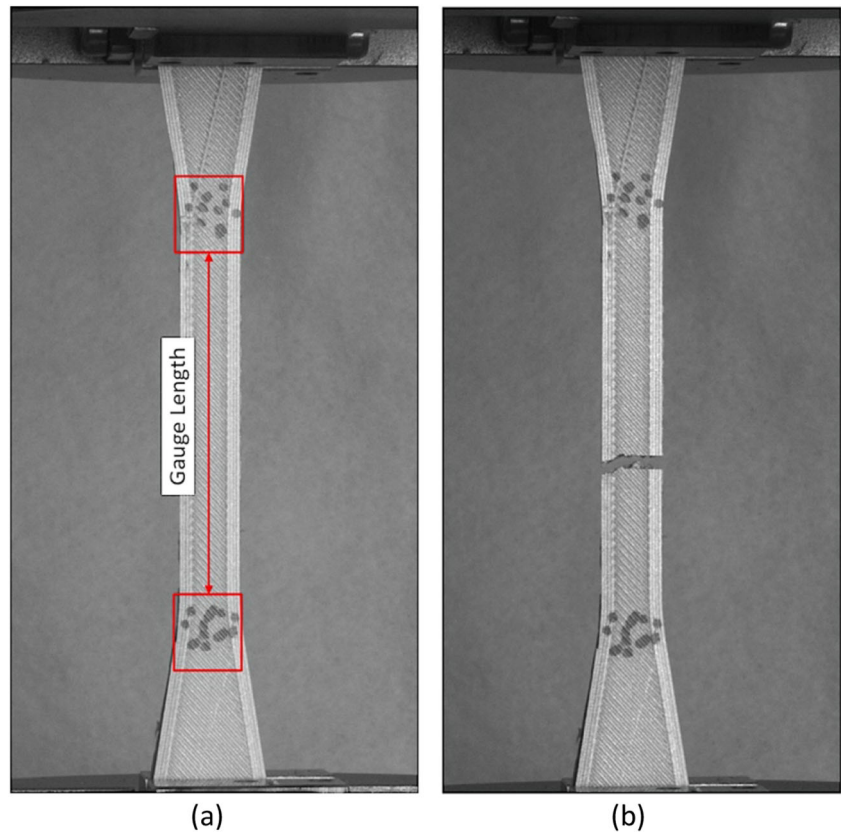(a)   (b)

Figure 7a shows the effect that the manufacturing parameters have on UTS. Increasing infill percentage, top/bottom layers and solid shells are all shown to increase UTS. Of these, the effect of infill percentage is highest with a 15 MPa difference between levels 1 and 3. Increasing layer height can be seen to have a negative effect on UTS. Build orientation (a categoric variable) is shown to impact UTS with specimens printed in the *Y*-direction (3 MPa) stronger than those in the *X*-direction and significantly stronger than those in the *Z*-direction (10 MPa).

Figure 7b demonstrates the effect that manufacturing parameters have on tensile modulus. The relationships are similar to those for UTS, with infill percentage, top/bottom layers

and solid shells all exhibiting positive relationships with tensile modulus and layer height a negative one. Tensile modulus is shown to be highest for specimens printed in the *Y*-direction and lowest in the *Z*-direction.

The directives of these relationships can be seen to be consistent with those in literature (as stated in Section 2.1) with positive correlations observed between infill percentage and solid shells with UTS and negative correlations with layer height. Part strength is also shown to be weakest in the *Z*-direction as also demonstrated in literature.

Agreement between experimental test results and those in literature supports their validity.
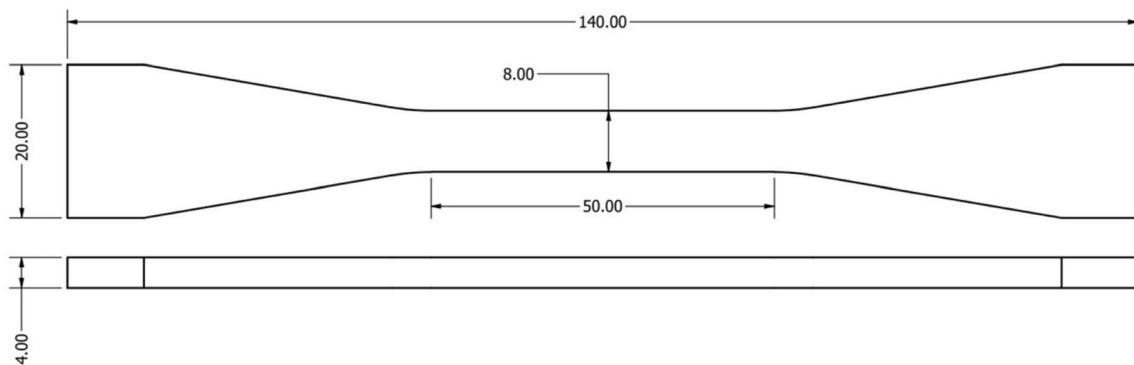

Fig. 5 Test specimen with key dimensions

Table 3 Test results from experimental testing. Ultimate tensile strength and tensile modulus are abbreviated to UTS and E, respectively

| Sample | | Measured parameters | | | | | | Calculated parameters | | | | | |
| | | Cross-sectional area (mm^2) | | Max load (kN) | | Extension (mm) | | UTS (MPa) | | % Strain at UTS | | E (GPa) | |
	n	Mean	SD	Mean	SD	Mean	SD	Mean	SD	Mean	SD	Mean	SD
1	6	32.09	0.01	0.64	0.01	1.16	0.17	19.83	0.44	1.75	0.27	1.35	0.05
2	6	33.23	0.01	1.24	0.02	1.56	0.23	37.39	0.67	2.23	0.29	2.54	0.09
3	6	32.71	0.26	1.35	0.02	1.33	0.23	41.31	0.53	2.04	0.30	3.28	0.14
4	6	33.48	0.28	0.89	0.04	1.18	0.13	26.74	1.35	1.90	0.25	1.95	0.06
5	6	33.42	0.44	1.11	0.05	1.05	0.11	33.30	1.26	1.70	0.13	2.65	0.25
6	6	32.04	0.42	1.55	0.09	1.01	0.05	48.39	3.11	1.67	0.08	3.20	0.03
7	4	32.14	0.15	0.25	0.01	0.61	0.02	7.88	0.22	1.00	0.03	0.91	0.01
8	6	30.80	0.39	1.22	0.07	0.89	0.07	39.72	2.31	1.48	0.09	3.05	0.09
9	6	33.37	0.09	1.39	0.03	1.03	0.05	41.55	1.14	1.82	0.09	2.95	0.16
10	4	32.17	0.18	1.66	0.03	1.36	0.66	51.54	1.07	2.37	1.17	3.46	0.20
11	5	31.79	0.35	0.63	0.31	0.66	0.32	23.53	0.26	1.34	0.06	2.33	0.03
12	5	30.38	0.93	1.32	0.06	0.86	0.43	43.49	0.83	1.93	0.13	3.02	0.09
13	6	31.30	0.23	1.12	0.09	0.97	0.16	35.86	2.88	1.73	0.26	2.54	0.08
14	6	33.88	0.04	0.92	0.02	1.14	0.06	27.22	0.68	1.97	0.11	2.08	0.06
15	6	33.52	0.15	1.00	0.01	0.93	0.11	29.83	0.47	1.71	0.15	2.46	0.09
16	5	33.43	0.15	0.51	0.06	0.69	0.13	15.26	1.85	1.28	0.26	1.77	0.06
17	6	30.13	0.23	0.69	0.12	0.63	0.14	22.78	3.90	1.17	0.26	2.30	0.03
18	6	33.25	0.25	1.43	0.03	1.13	0.04	43.06	0.72	1.99	0.08	3.08	0.06
19	5	32.93	0.22	2.03	0.05	1.06	0.01	61.61	2.15	1.91	0.18	4.12	0.28
20	6	29.62	0.36	2.97	0.04	1.28	0.09	100.24	1.05	2.28	0.19	6.40	0.21
21	6	33.13	0.14	1.49	0.05	0.62	0.04	44.89	1.39	1.11	0.09	4.25	0.37

6 Capability profiling

This section details the process of generating a capability profile from the experimental data.

6.1 Method

Artificial neural networks (ANNs) were selected as a method for generating a predictive model. The advantages of predictive
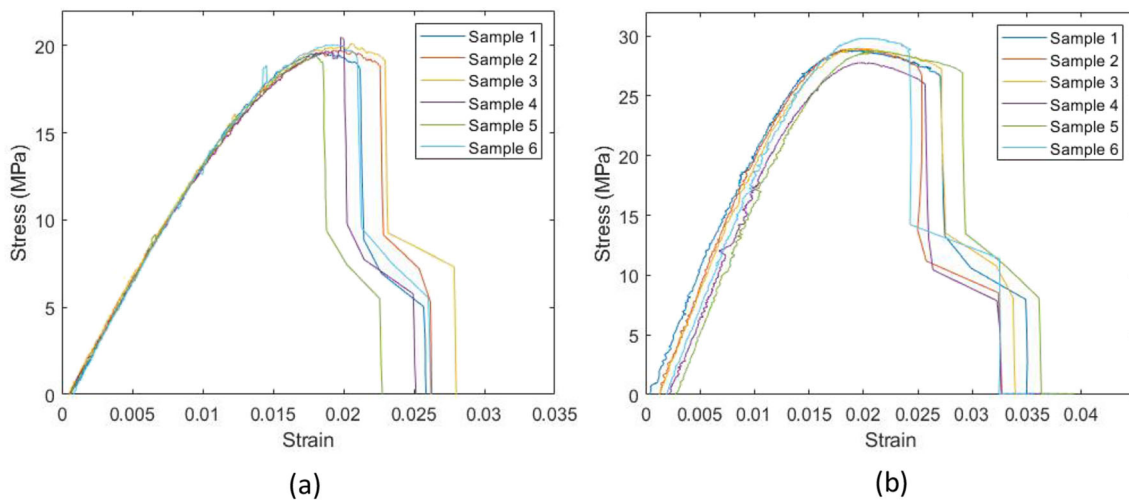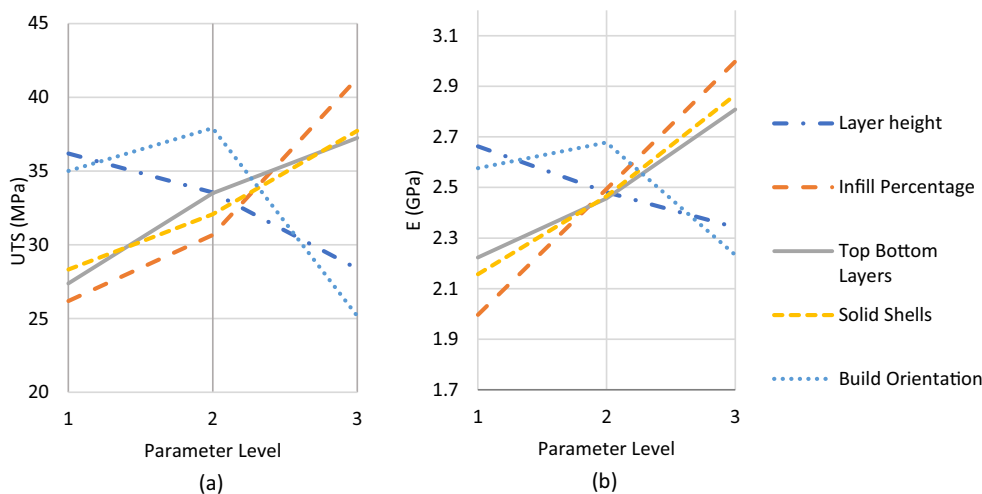

Fig. 6 Stress-strain curves from material testing—**a** parameter set 1, **b** variable set 14

Figure 7 Graphs demonstrating the normalised impact of each variable on **a** ultimate tensile strength (UTS) and **b** tensile modulus (*E*)

(a)

(b)

— · — Layer height

– – – Infill Percentage

———— Top Bottom Layers

– – – Solid Shells

·········· Build Orientation

modelling through the use of neural networks include their ability to detect all possible interactions between independent variables and their implicit ability to detect complex non-linear relationships. This is achieved through a black-box and as such a drawback of this exists in there being limited ability for identification of possible causal relationships [42]. The use of this technique was deemed suitable for the sample size of (120) due to previous applications of ANNs in FDM property prediction and for similar sample sizes (144) [29].

IBM SPSS 24 was used to generate a predictive model via use of a multi-layer perceptron neural network. The data was auto-partitioned with 60% of the data used for training, 20% for test and 20% hold-out categories. All 21 sets of data were pooled together yielding a total of 120 samples. Stopping criteria for the network was set at 1000 steps passing without improvement in performance with a minimum relative change in training error of 0.0001. The loss function was calculated by backpropagation as sum of squares error from the scaled conjugate gradient method. Batch training was used to generate the neural network as it is generally preferred method of training as it directly minimises total error and is most suitable for 'smaller' datasets [43].

A single hidden layer was used in the neural networks as this 'can approximate any function that contains a continuous mapping from one finite space to another' [44]. The activation function of this hidden layer was hyperbolic tangent. The number of nodes within this neural network was decided upon automatically by the SPSS software. Automatic architecture selection in SPSS computes the 'best' number of units in the hidden layer. Maximum and minimum values for neurons in the hidden layer were bounded by 50 and 1, respectively.

6.2 Results

Using the settings outlined in the previous section, four neural networks were generated as potential capability profiles for FDM. Their performance was assessed and that which was best

able to predict mechanical properties of UTS and tensile modulus was selected for use in the capability profile. The feedforward architecture of the network is shown in Fig. 8 and respective synapse weights are shown in Table 5. The predictive power of this is demonstrated by Fig. 9 with respect to predictive vs. actual values. The graphs demonstrate acceptable predictive power across the ranges of values for UTS and *E*. Route mean square error of prediction (RMSEP) for all data is calculated as 1.95 MPa for UTS and 0.82 GPa for *E*—both within acceptable bounds for predicting 3D-printed part behaviours. Relative predictive errors are shown in Table 4 for training, test and holdout data for both UTS and *E* and are also within acceptable bounds.

7 Integrating the capability profile in a generative design methodology

Whilst the predictive ability of the capability profile has been demonstrated, to validate its usability, it will be applied in the design of two load bearing components via means of a generative methodology that can enable design support. It is achieved by enabling the generation of functional components without the designer needing requisite knowledge of the FDM process or static mechanics. As it is beyond the scope of this paper to describe the methodology in depth, what follows is a brief overview with particular attention given to the role the capability profile plays within it. Two instantiations of the methodology are then

Table 4 Relative predictive error of UTS and *E* for training, test and holdout data

Training		Test		Holdout	
UTS	*E*	UTS	*E*	UTS	*E*
0.8%	1.3%	4.0%	3.7%	1.2%	2.4%

Fig. 8 Feedforward architecture of ANN underpinning capability profile (synapse weights are shown in Table 5)
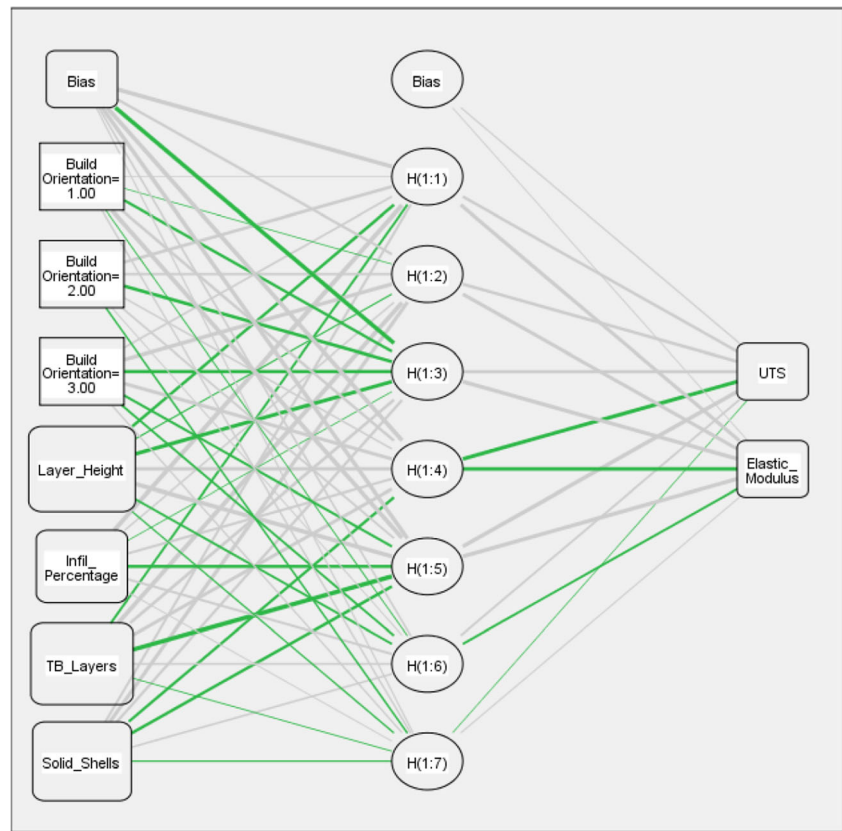
presented to illustrate its use, for a more detailed overview of the methodology and its workings see [45].

7.1 Methodology overview

The design methodology fuses design activities from both physical and virtual domains. Via simulation in the virtual domain, a design of a satisfactory part is generated. The part is then manufactured and is physically tested to either validate its behaviour or identify functional shortcomings. If the part is hitherto unsatisfactory, the test results are incorporated into the next round of simulation to permit the generation of an improved part. This iterative process is continued until a satisfactory part is produced. The process is summarised in Fig.
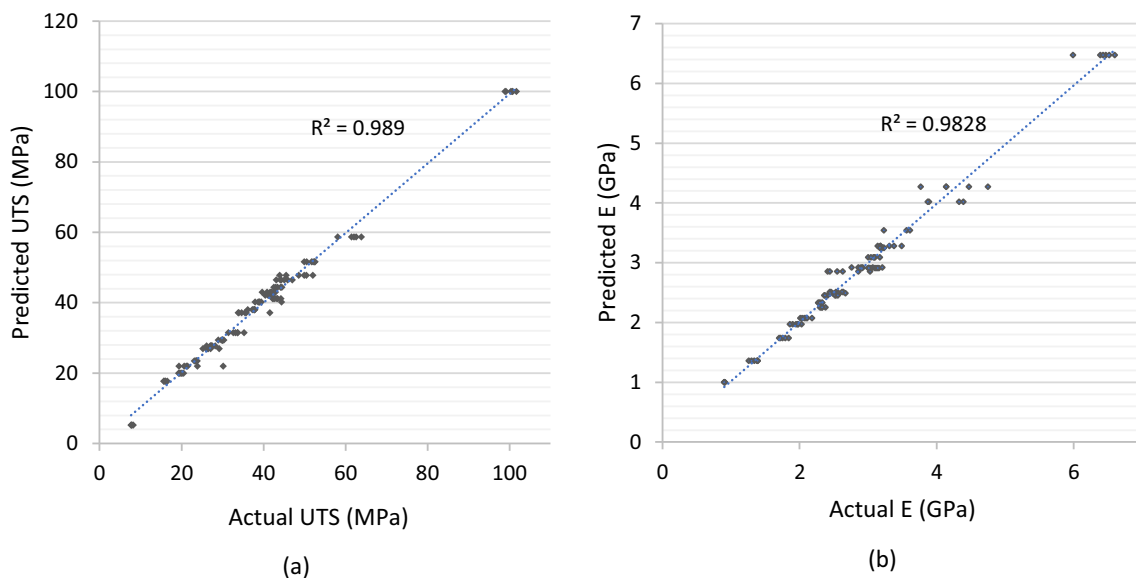
Fig. 9 ANN-predicted values vs actual values for **a** ultimate tensile strength (UTS) and **b** tensile modulus (*E*)

10 which is colour coded in accordance with the process that each activity is carried out. It leverages quick iteration in the virtual domain with accurate testing in the physical to enable the generation of functional components. The methodology is explained by first defining the solution space and then how it is explored to find a design solution.

7.1.1 Defining the solution space

Part behaviour is determined via simulation which corresponds to stage 3 in Fig. 10. The three key elements that enable this to happen are a capability profile, a functional model and a structural parametric model. Their respective roles are shown in the form of an agent-based representation in Fig. 11 and can be elaborated upon as follows.

The capability profile interrelates manufacturing parameters with a part's mechanical properties. This is achieved by re-representing the ANN (detailed in Fig. 8 and Table 5) which enables the conversion of input manufacturing parameters to UTS and tensile modulus.

The capability profile underpins a functional model. This is able to deduce emergent functional behaviour of the part (such as load bearing capacity) through coupling its mechanical properties with shape properties (e.g. area and second moment of area) geometry. This is achieved by calculating the predicted load a part is able to sustain via classical analysis techniques. This approach is similar to that used by Umetani et al. to identify weak elements in prints in order to optimise
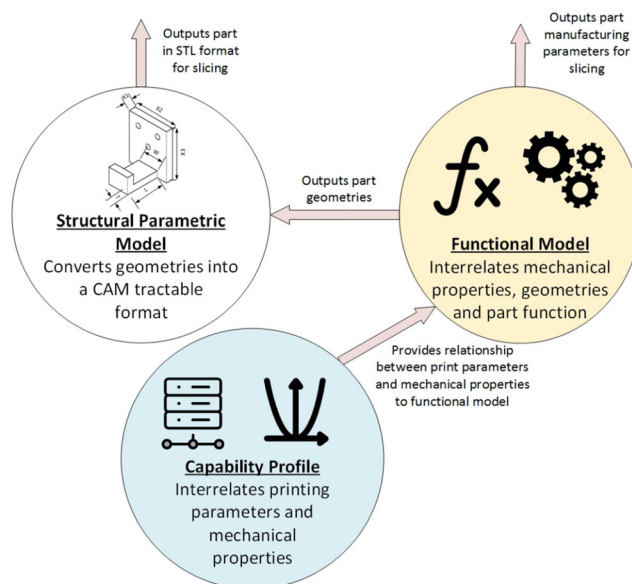
Fig. 11 Agent-based representation of how part behaviour is simulated within the design methodology, demonstrating how the capability profile fits within it.

build orientation [46]. A structural parametric model then converts these geometries and outputs the design in a CAD tractable format. Finally, this can then be combined with manufacturing parameters to allow the creation of a manufacturing instruction.

7.1.2 Exploration of the solution space

The design parameters (as shown in Fig. 12) define the solution space in which a satisfactory design can be generated. Particle swarm optimisation (PSO) is used to navigate this solution space and generate a design solution. PSO was selected as it was shown in previous work to outperform evolutionary algorithms and simulated annealing in the context of manufacturing parameter selection for FDM by producing better and less varied results [5]. This optimisation process is directed by a fitness function that seeks to sustain a given load whilst minimising material usage and ensuring that a manufacturable part is generated.

7.1.3 Implementation

The methodology is implemented within Rhinoceros 6's Grasshopper [47] add-on. An example implementation is shown in Fig. 12. A designer using this methodology needs to input their load requirement and physical testing results (shown as user input parameters in Fig. 12).

The solution space is defined by the capability profile and functional modelling (comprising load calculation and shape analysis in Fig. 12).
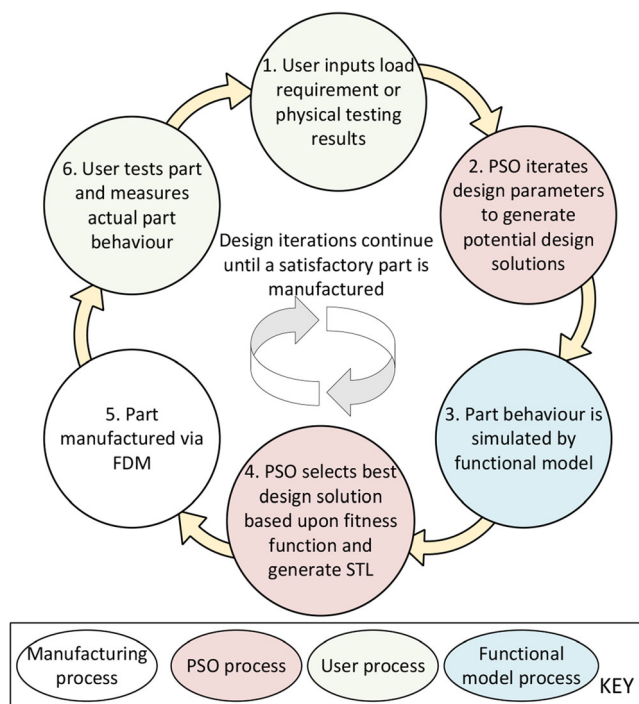

Fig. 10 Overview of iterative design process. Acronyms are defined as particle swarm optimisation (PSO), standard Triangle language file type (STL) and filament deposition modelling (FDM)

Table 5 Synapse values from ANN - Build orientation is abbreviated to BO

Predictor		Hidden layer							Output layer	
		H(1:1)	H(1:2)	H(1:3)	H(1:4)	H(1:5)	H(1:6)	H(1:7)	UTS	EM
Input layer	Bias	1.628	0.668	− 1.70	1.83	1.543	0.256	0.166		
	BO1	.062	− .031	− .74	.758	2.03	− .132	.203		
	BO2	.979	0.663	− .994	.22	.37	.16	− .25		
	BO3	.257	1.317	− 1.05	1.13	− .56	− .48	.20		
	LH	− .79	− .157	− 1.24	1.19	1.87	− .49	− .19		
	Infill	2.63	0.21	− .06	0.66	− .90	.51	.14		
	TB_Layers	− .497	2.24	.86	1.01	− 2.31	.31	− .06		
	Solid shells	.62	1.24	.71	− .71	− .85	.25	− .19		
Hidden layer	Bias								.19	.12
	H(1:1)								.78	1.22
	H(1:2)								.94	1.17
	H(1:3)								.99	1.32
	H(1:4)								− 1.28	− 1.2
	H(1:5)								1.39	1.34
	H(1:6)								0.40	− .49
	H(1:7)								− .03	.16

Grasshopper's silvereye PSO solver is used to explore the solution space and find a solution. It iterates through the design parameters of height and width (at load bearing cross-section), build orientation, layer height, infill percentage, top/bottom layers and solid shells (shown as design parameters in Fig. 12) to find the best design solution.

7.2 Applying the methodology to design tasks

Two design tasks were carried out with the design methodology. These were a tensile specimen and an S-hook which were both designed to withstand a pre-determined load. The setup of each design problem in Grasshopper took between 1 and 2 h. Each particle swarm optimisation lasted roughly 1 min. Whilst seemingly simple design tasks, they embody a number of the complexities that arise when considering design for AM. The design freedoms afforded enable, for example, maximisation of strength with minimum material usage. However, when trying to increase the strength of parts, it is unclear if this is best achieved by increasing the cross-sectional area, amending the manufacturing parameters or a mixture of both. The methodology above, underpinned by the
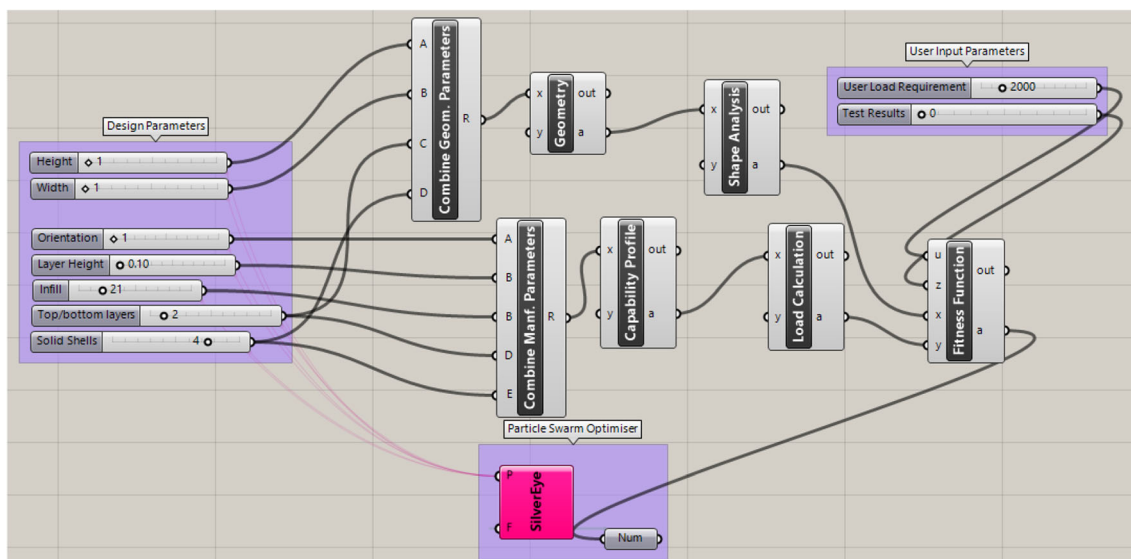

Fig. 12 Implementation of functional model of generative design methodology within Grasshopper demonstrating solution space definition

capability profile generated in this paper, can be used to make these decisions in place of the user.

The generated tensile specimen is shown in Fig. 13a and was to be designed to have a break load of 1.5 kN. The specimen's dimensions and manufacturing parameter inputs are shown in Fig. 13b. Its predicted break load was calculated by multiplying the predicted UTS generated by the capability profile with its cross-sectional area. Three tensile specimens were generated iteratively with different manufacturing parameters and cross-sectional areas. These were tested to break with an Instron 8872. The input parameters for these specimens along with their predicted and actual performance are shown in Table 6. Three iterations were required in order to meet the part's functional requirement of sustain a 1.5 kN load.

The bending use case was an S-hook, had a target break load of 150 N. It was selected as a commonly manufactured, functional 3D-printed component [48]. Its key dimensions are shown in Fig. 14a and functional testing is depicted in Fig. 14b. The parameters varied during the iteration are shown in Table 6.

The part's functional model predicted its break load, which was calculated by deducing bending stress (σ) through use of Euler-Bernoulli beam theory [49] as shown in Eq. 1

$$\sigma = \frac{My}{I} \qquad (1)$$

where M is the applied moment, y the distance from the neutral axis, I is the second moment of area. Second moment of area of the hook is calculated through the summation of second moment of area of the infill and solid shells which are shown as the white and grey areas in Fig. 13b, respectively.

Two iterations were required to meet the part's functional requirement. These are shown in Table 6.

The performance of the capability profile can be seen to overestimate the mechanical performance of the parts with the ratio of actual to predicted load between 0.51 and 0.63 for the tensile specimen and of 0.86 for the S-hook. In spite of these over predictions, these examples have demonstrated that the methodology can enable the generation of functional parts with pre-requisite knowledge of neither FDM nor static mechanics through the combination of activities from virtual and physical design domains.

The observed over-predictions in the functional modelling approach could be attributed to a number of different elements. These along with potential remedies will be detailed in Section 8.2.

8 Discussion and further work

This paper has presented the generation of a capability profile and its subsequent implementation within a generative design

Table 6 Results of generated parts. Iteration is abbreviated to It

Parameters	Tensile specimen			S-hook	
	It. 1	It. 2	It. 3	It. 1	It. 2
Build orientation	X	X	Y	X	X
Height (mm)	11.1	5.3	13.3	4	4
Width (mm)	2.3	7.2	4	14	15
Infill (%)	80	59	68	79	81
Solid shells (#)	7	3	2	2	4
TB layers (#)	7	8	5	6	6
Layer height (mm)	0.22	0.17	0.3	0.3	0.3
Predicted load (kN)	1.50	2.25	2.9	0.15	0.174
Actual load (kN)	0.94	1.15	1.61	0.13	0.15
Ratio of actual/predicted	0.63	0.51	0.56	0.867	0.863

methodology has demonstrated that it can enable the creation of functional load-bearing components. As such, the research aim of the paper has been met.

To consider the implications of this, the following discussion section will appraise the experimental method for developing the capability profile, how its performance could be improved, the benefits of coupling physical and virtual methods within design processes, and more widely consider the generalisability of both capability profiles for FDM and the presented design methodology. In doing this, it provides recommendations as to how future implementations of similar approaches for FDM could be improved.

8.1 Experimental method for developing the capability profile

The experimental testing was carried out in accordance with the relevant ASTM standard but with the test sample used featuring an amended cross-section in order to accommodate a range of values for the manufacturing parameters that were varied. The need to do this highlights a necessary research gap. Current testing standards seek to enable the elucidation of the mechanical properties of materials. However, in additive manufacturing, as many parameters directly influence these properties, referring to the mechanical properties of materials becomes a red herring as it constitutes only a small piece of the puzzle regarding the mechanical properties of AM parts. It is therefore necessary that testing standards specific to additive manufacturing techniques are developed. These would need to contain a range of specimen sizes that would permit enough variation of different manufacturing parameters in order to measure the effect that these have on mechanical properties. The development of such test standards represents a step for further work, to be undertaken in
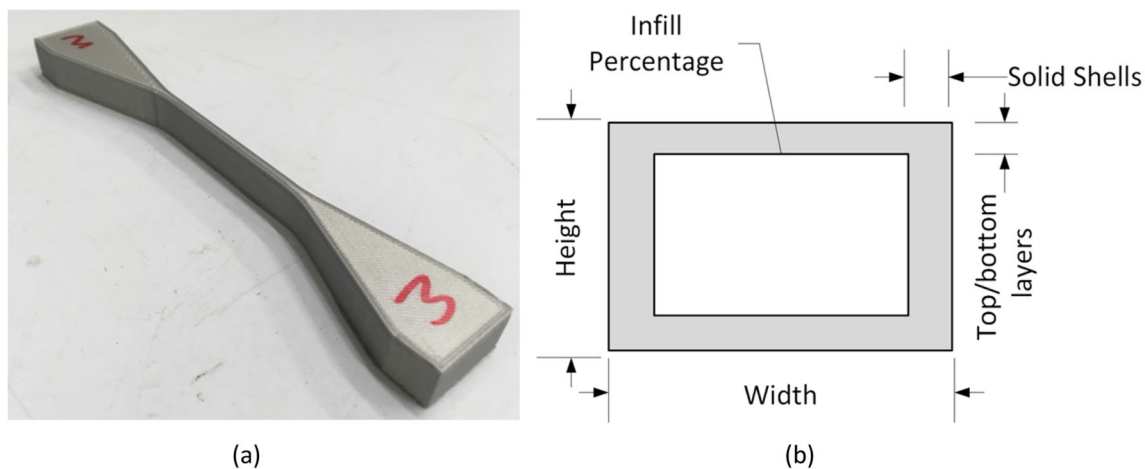
Fig. 13 Tensile use case **a** sample-generated test specimen, **b** tensile test specimen cross-section with input parameters

collaboration with other stakeholders such as researchers and manufacturers in the 3D printing community.

## 8.2 The performance of the capability profile

The predicted vs. actual values of the capability profile for both UTS and E showed good correlation in Section 6.2. But discrepancies in the form of over-estimation were observed when the capability profile was applied via the generative methodology in actual design tasks. This could be due to a number of factors, such as the generation of parts outside of the training data range of the ANN, overfitting or inaccuracies in the functional modelling approach.

A key limitation in the use of ANNs to form the capability profile is that they cannot predict reliably if extrapolating beyond the training data used in its generation [50]. When using

the generated capability profile therefore, input manufacturing parameters should not greatly exceed those used in its generation. In the tensile use case, the target load is 1.5 kN which is towards the upper bounds of the training data and therefore predictive range of the generated ANN. This is a limitation which must be considered during the capability profile's implementation so as to mitigate against inaccurate predictions. On reflection, better performance could perhaps be enabled by either generating parts with lower load bearing capacities, or expanding the capability profile with higher load specimens.

Whilst the sample size used for this study was similar to others in literature that use ANNs as predictive models for additive manufacture, in the wider context of machine learning, the sample size is relatively small. This coupled with the repeat tests necessary for each sample gives rise to the risk of overfitting occurring in the ANN, which could account for the

Fig. 14 Bending use case **a** S-hook annotated with key dimensions, **b** functional testing of S-hook
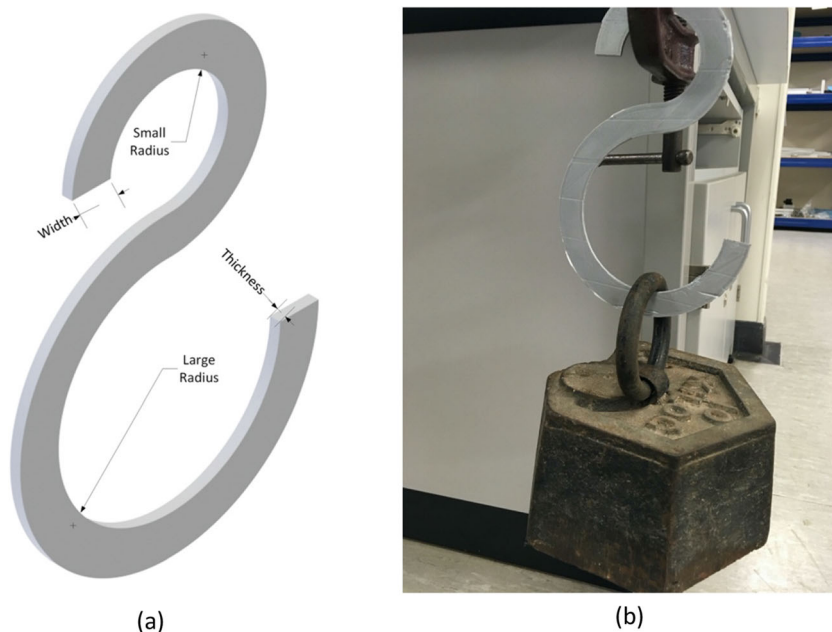
discrepancies between the components' actual and predicted behaviours. This can be mitigated in future work by using larger data sets and techniques such as regularisation and cross-validation when using ANNs.

The functional modelling approach could also account for discrepancies between predicted and actual behaviours of the parts generated. This modelling defines to what extent the PSO is able to converge on a solution. For the bending use case due to the incorporation of second moment of area providing additional bounds to the solution space, convergence towards a specific shape is observed with consistencies across iterations. For the tensile use case, however, as second moment of area is not included, there are no specific constraints on where material is added resulting in less consistent results suggesting the PSO could be finding local rather than global maxima. Both of these examples were idealised in that they described parts under pure tension or bending. In reality, parts need to stand a combination of loading (e.g. tension, bending torsion and shear); as such, future functional modelling would need to incorporate a combination of these to facilitate a better bounded solution space to aid in the prediction of part performance.

Evaluating the performance of the capability profile also requires us to consider whether the five parameters selected were the right ones to include. The results of experimental data shown in Figure 7 (Section 5.1) demonstrate considerable impact of the selected parameters on both UTS and tensile modulus. This indicates that they are the right parameters to include as they significantly impact mechanical properties and therefore part function. It may be that additional parameters (such as print speed or extruder temperature) need to be incorporated and as such this is a considered item of further work.

In addition, whilst these parameters are predicted by the capability profile, additional consideration is necessary to determine if an individual manufacturing resource is able to guarantee the value of the five parameters used. This requires an addition of an extra step to the methodology in the form of analysis of the as sliced geometry in the form of the G-code toolpath. A comparison of the as sliced geometry with the intended geometry and manufacturing parameters would permit elucidation if the delta between these is significant and if so, re-calculation of predicted performance could be carried out before manufacture.

8.3 The benefits of physical and virtual design coupling

The presented design methodology demonstrated the benefits of coupling digital and physical design activities. Virtual activities via means of generative approaches allow rapid exploration of the FDM solution space and the generation of designs optimised for 3D printing. Both use cases shown in Section 7.2 demonstrate the exploration of a 7-dimensional design space in minutes, an undertaking which could not be

carried out in the physical domain. On the other hand, the physical domain allows real world validation of theoretical part performance which, as highlighted in Section 2.1, is necessary as the FDM process is at present insufficiently understood to allow this to be reliably predicted. The two elements work together synergistically to enable the generation of functional parts. This coupling of virtual and physical domains makes the methodology relevant as from a design perspective, hybrid virtual-physical methodologies such as these are essential in enabling the manufacture of functional 3D-printed parts. Moreover, 3D printing permits the rapid manufacture of parts meaning that this necessary physical validation is an expedient and affordable process.

An additional benefit observed from this physical virtual coupling is the reduction in skill level that a user requires in order to create a functional part. It enables automation of elements of the design for FDM process and subsequently reduces design difficulty. Extant design tools in this space include Autodesk's Design Automation [51]. Future work is to characterise this and understand the specific manner in which this is enabled by the presented generative methodology. This will be undertaken using an extant methodology for assessing process difficulty from literature [52].

8.4 Generalisability

The generalisability of the work presented considers two elements, that of using ANNs as capability profiles and of the design methodology on the whole.

The extensive experimental testing presented in this paper is not a practical approach for everyone to follow in order to create individual capability profiles for their own printers. But there are ways this could be worked around to make the use of capability profiles more straightforward. More general capability profiles could be tailored to an individual manufacturing resource via physical benchmarking processes. Further work would then look at how a capability profile for one printer could be translated to another. Once a capability profile was mapped and validated (as proposed in Section 8.2) for some arbitrary printer A, work could look at how many test results from printer B are required to satisfactorily adapt the capability profile of printer A to permit the formation of a capability profile for printer B.

With respect to the overall methodology, the incorporated element of physical testing presents a number of opportunities for design learning following Confucius' three methods of acquiring wisdom: experience, imitation and reflection [53].

Initial use of the design methodology (as demonstrated in this paper) will require users to directly engage in virtual-physical iterations in order to arrive at a suitable part. However, as identical parts are manufactured by different users, process knowledge grows and lessons learned from the different design cycles are able to inform the decisions taken for the

next design of the same part. In this way, if a different user wished to make the same part, through imitation (i.e. use of existing knowledge), their design experience can be quicker and easier. This accumulated design knowledge can also be applied to different design tasks. Elements of that which is learned in the design of part A can be applied to parts B and C. This can be viewed as learning by reflection as knowledge is transferred across domains to permit the design or different parts. This is the global learning undertaken across all designs using the design methodology. The ascertained knowledge can be pooled to make evermore effective models of the FDM process and refine the dynamic models themselves.

This enables something conceptually similar to Communities of Practice, of which the purpose is to 'develop members' capabilities, to build and exchange knowledge' [54]. In the context of design for additive manufacturing, the global design learning afforded by the wider implementation of the design methodology enables a community of practice, with users learning from each other's design experiences.

A longer-term goal for further work is therefore to apply the methodology more widely to enable the Confucian learning modes of imitation and, ultimately, reflection. This could be carried out by implementing the design methodology within a design library such as Thingiverse [55].

An additional avenue for further work involves the incorporation of build time into the capability model. The application of the methodology featured an optimisation of mechanical performance against material usage. Build time would also be valuable to include as it is significantly impacted by a number of manufacturing parameters [56] and also impacts design and manufacturing decisions, particularly when prototyping [57]. This could be achieved by first following a similar methodology as presented by Hallman et al. to carry out a sensitivity analysis as to which parameters most significantly impact build time [56]. This could then be coupled with methodology for capability profile generation presented in this paper incorporating any additional parameters that would be necessary to create an ANN that would be able to predict both mechanical properties and build time. An appropriate objective function would then need to be implemented to account for the relative magnitudes of a designer's manufacturing restrictions in terms of material use or build time. This would likely require inclusion of print speed which as well as impacting build time would also effect

9 Conclusion

The paper is concerned with creating a capability profile that can be used as part of a generative design process in order to enable leveraging of FDM affordances with respect to individually controlling manufacturing parameters to create parts with bespoke properties.

The literature review highlighted the need to (i) conduct comprehensive testing on a single printer, (ii) incorporate parameters previously omitted from extant capability profiles for FDM, (iii) validate the behaviour of a capability profile by applying it to the creation of functional components and (iv) implement the capability profile within a generative design approach. These needs defined the research gaps and the approach that would be followed in generating and applying a formal model to capture the capabilities of FDM machines.

To generate capability profiles, a comprehensive set of mechanical tests was undertaken on parts made on a single printer. A Taguchi approach was applied in accordance with ASTM standards and featured 120 samples and five parameters consisting of layer height, build orientation, solid shells, top/bottom layers and infill percentage each varied at three levels each. The experimental data was validated with respect to existing literature.

The experimental data was used to train an Artificial Neural Network (ANN) forming the basis of a capability profile for FDM with route mean square error of prediction (RMSEP) for all data of 1.95 MPa for UTS and 0.82 GPa for E. These values which are well within the acceptable range for many popular uses of FDM generated parts.

To validate the performance and utility of the capability profile, it was incorporated within a generative design approach that iteratively fuses activities from both physical and virtual domains. In the design of two functional parts, it was shown to over-predict part performance with the ratio of actual to predicted performance of parts between 0.6 and 0.8. However when coupled with physical validation of parts, it enabled the generation of parts to meet functional requirements in 2–3 design iterations—more quickly and reliably than a manual approach.

Possible causes of predictive discrepancies of the capability profile include the selection of use cases towards the edge of the ANN's predictive ability and potential sub-optimal bounding of the solution space through the functional modelling approach employed. Further work will involve refinement in both of these areas as well as investigating the incorporation of build time into the overall approach. The benefits of fusing virtual and physical design domains are also presented reinforcing the validity of the generative methodology. The generalisability of the presented approach is also considered with respect to its longer-term vision and application within design repositories in order to create a community of practice.

Declarations

References

1. Attaran M (2017) The rise of 3-D printing: the advantages of additive manufacturing over traditional manufacturing. Bus Horiz 60(5):677–688
2. Knofius N, van der Heijden MC, Zijm WHM (2019) Moving to additive manufacturing for spare parts supply. Comput Ind 113:103134
3. Berman B (2012) 3-D printing: the new industrial revolution. Bus Horiz 55(2):155–162
4. Foresight (2015) The future of manufacturing: a new era of opportunity and challenge for the UK
5. Goudswaard M, Nassehi A, Hicks B (2019) Towards the democratisation of design : the implementation of metaheuristic search strategies to enable the auto-assignment of manufacturing parameters for FDM. In: Proceedings of the International Conference on Flexible Automation and Intelligent Manufacturing, vol 00
6. Holst A. Worldwide most used 3D printing technologies, as of July 2018, Statista, 2018. [Online]. Available: https://www.statista.com/statistics/756690/worldwide-most-used-3d-printing-technologies/. Accessed: 02-Jul-2019
7. Gebler M, Schoot Uiterkamp AJM, Visser C (2014) A global sustainability perspective on 3D printing technologies. Energy Policy 74(C):158–167
8. Popescu D, Zapciu A, Amza C, Baciu F, Marinescu R (2018) FDM process parameters influence over the mechanical properties of polymer specimens: a review. Polym Test 69(April):157–166
9. Goudswaard M, Hicks B, Nassehi A (2020) Towards the democratisation of design: a generalised capability model for FDM. Int J Agil Syst Manag 13(1)
10. Tymrak BM, Kreiger M, Pearce JM (2014) Mechanical properties of components fabricated with open-source 3-D printers under realistic environmental conditions. Mater Des 58:242–246
11. Onwubolu GC, Rayegani F (2014) Characterization and optimization of mechanical properties of ABS parts manufactured by the fused deposition modelling process. Int J Manuf Eng 2014:1–13
12. Sood AK, Ohdar RK, Mahapatra SS (2012) Experimental investigation and empirical modelling of FDM process for compressive strength improvement. J Adv Res 3(1):81–90
13. Lanzotti A, Grasso M, Staiano G, Martorelli M (2015) The impact of process parameters on mechanical properties of parts fabricated in PLA with an open-source 3-D printer. Rapid Prototyp J 21(5):604–617
14. Zhao Y, Chen Y, Zhou Y (2019) Novel mechanical models of tensile strength and elastic property of FDM AM PLA materials: experimental and theoretical analyses. Mater Des 181:108089
15. Garzon-Hernandez S, Garcia-Gonzalez D, Jérusalem A, Arias A (2020) Design of FDM 3D printed polymers: an experimental-modelling methodology for the prediction of mechanical properties. Mater Des 188:108414
16. Alafaghani A, Qattawi A, Alrawi B, Guzman A (2017) Experimental optimization of fused deposition modelling processing parameters: a design-for-manufacturing approach. Procedia Manuf 10:791–803
17. Chacón JM, Caminero MA, García-Plaza E, Núñez PJ (2017) Additive manufacturing of PLA structures using fused deposition modelling: effect of process parameters on mechanical properties and their optimal selection. Mater Des 124:143–157
18. Croccolo D, De Agostinis M, Olmi G (2013) Experimental characterization and analytical modelling of the mechanical behaviour of fused deposition processed parts made of ABS-M30. Comput Mater Sci 79:506–518
19. Sood AK, Ohdar RK, Mahapatra SS (2010) Parametric appraisal of mechanical property of fused deposition modelling processed parts. Mater Des 31(1):287–295
20. Casavola C, Cazzato A, Moramarco V, Pappalettere C (2016) Orthotropic mechanical properties of fused deposition modelling parts described by classical laminate theory. Mater Des 90:453–458
21. Wittbrodt B, Pearce JM (2015) The effects of PLA color on material properties of 3-D printed components. Addit Manuf 8:110–116
22. Zhang J, Wang XZ, Yu WW, Deng YH (2017) Numerical investigation of the influence of process conditions on the temperature variation in fused deposition modeling. Mater Des 130(March):59–68
23. Goudswaard M, Hicks B, Nassehi A (2018) Towards the democratisation of design : exploration of variability in the process of filament deposition modelling in desktop additive manufacture. Proc. Conf. Transdisciplnary Eng.
24. Newman ST, Nassehi A (2009) Machine tool capability profile for intelligent process planning. CIRP Ann Manuf Technol 58(1):421–424
25. Klocke F, Brinksmeier E, Weinert K (2005) Capability profile of hard cutting and grinding processes. CIRP Ann Manuf Technol 54(2):22–45
26. Vichare P, Nassehi A, Thompson J, Newman ST, Wood F, Kumar S (2015) Machine tool capability profiles for representing machine tool health. Robot Comput Integr Manuf 34:70–78
27. Bartarya G, Choudhury SK (2012) State of the art in hard turning. Int J Mach Tools Manuf 53(1):1–14
28. Meng L, McWilliams B, Jarosinski W, Park HY, Jung YG, Lee J, Zhang J (2020) Machine learning in additive manufacturing: a review. Jom 72(6):2363–2377
29. Zhang J, Wang P, Gao RX (2019) Deep learning-based tensile strength prediction in fused deposition modeling. Comput Ind 107:11–21
30. Pieters R, Winiger S (2016) On the Democratisation & Escalation of Creativity, Medium.com. [Online]. Available: https://mediumcom/@creativeai/creativeai-9d4b2346faf3. Accessed: 06-Dec-2017

31. Shneiderman B (2000) Creating creativity: user interfaces for supporting innovation. ACM Trans Comput Interact 7(1):114–138

32. Hansmeyer M (2012) Building Unimaginable Shapes, Ted Global 2012. [Online]. Available: https://www.ted.com/talks/michael_hansmeyer_building_unimaginable_shapes

33. Autodesk Inc, Generative Design (2019) [Online]. Available: https://www.autodesk.com/solutions/generative-design. Accessed: 19-Jul-2019

34. Trinckle, Paramate (2019) [Online]. Available: https://www.trinckle.com/en/enterprise/paramate.php

35. Silva FJG, Campilho RDSG, Gouveia RM, Pinto G, Baptista A (2018) A novel approach to optimize the design of parts for additive manufacturing. Procedia Manuf 17:53–61

36. V. Megaro, B. Thomaszewski, and M. Gross, Interactive design of 3D-printable Robotic Creatures, 2015

37. Prévost R, Whiting E, Lefebvre S, Sorkine-Hornung O (2013) Make It Stand: Balancing Shapes for 3D Fabrication. ACM Trans Graph 32(4):81:1–81:10

38. Bächer M, Whiting E, Bickel B, Sorkine-Hornung O (2014) Spin-it: optimizing moment of inertia for spinnable objects. ACM Trans Graph 33(4):96:1–96:10

39. Ranjit R (2010) A primer on the Taguchi method. Society of Manufacturing Engineers

40. Cimbala MJ (2014) Taguchi orthogonal arrays, Instrumentation, Measurements, and Statistics, no. September. pp 4–6

41. ASTM International (2003) D638 - Standard test method for tensile properties of plastics. ASTM Int 08:46–58

42. Schmidhuber J (2015) Deep Learning in neural networks: an overview. Neural Netw 61:85–117

43. IBM SPSS (2013) IBM SPSS Neural Networks 22

44. Heaton J (2017) The Number of Hidden Layers. [Online]. Available: https://www.heatonresearch.com/2017/06/01/hidden-layers.html. Accessed: 28-Aug-2019

45. Goudswaard M, Hicks B, Nassehi A (2018) Democratising the design of 3D printed functional components through a hybrid virtual-physical design methodology. Procedia CIRP 78:394–399

46. Umetani N, Schmidt R (2013) Cross-sectional structural analysis for 3D printing optimization, SIGGRAPH Asia 2013 Tech. Briefs, SA 2013

47. Rutten D (2019) Grasshopper 3D

48. Field Ready (2016) IV Bag Hook, Thingiverse. [Online]. Available: https://www.thingiverse.com/thing:1562085. Accessed: 11-Oct-2019

49. Timoshenko SP, Goodier JN, Abramson HN (1970) Theory of elasticity (3rd ed.). J Appl Mech

50. Trask A, Hill F, Reed S, Rae J, Dyer C, Blunsom P (2018) Neural arithmetic logic units. Adv Neural Inf Proces Syst 2018-Decem: 8035–8044

51. Autodesk Inc, Design Automation (2020) [Online]. Available: https://www.autodesk.co.uk/solutions/design-automation. Accessed: 17-Dec-2020

52. Goudswaard M, Hicks B, Gopsill J, Nassehi A (2017) Democratisation of design for functional objects manufactured by fused deposition modelling (FDM): lessons from the design of three everyday artefacts. ICED 2017 Conf Proc 5(August):219–228

53. Confucius (1979) The Analects. Penguin

54. Wenger E, Snyder W (2000) Communities of practice: the organizational frontier. Harcard Bus Rev

55. MakerBot (2019) MakerBot Thingiverse. [Online]. Available: https://www.thingiverse.com/. Accessed: 10-Jul-2019

56. Hallmann M, Schleich B, Wartzack S (2019) A method for analyzing the influence of process and design parameters on the build time of additively manufactured components. Proc Des Soc Int Conf Eng Des 1(1):649–658

57. Wall MB, Ulrich KT, Flowers WC (1992) Evaluating prototyping technologies for product design. Res Eng Des 3(3):163–177